Mathematical Modelling and Numerical Analysis
Modélisation Mathématique et Analyse Numérique

ESAIM: M2AN
M2AN, Vol. 36, N° 2, 2002, pp. 223–239
DOI: 10.1051/m2an:2002012

AN OPTIMUM DESIGN PROBLEM IN MAGNETOSTATICS*

Antoine Henrot[1] and Grégory Villemin[2]

Abstract. In this paper, we are interested in finding the optimal shape of a magnet. The criterion to maximize is the jump of the electromagnetic field between two different configurations. We prove existence of an optimal shape into a natural class of domains. We introduce a quasi-Newton type algorithm which moves the boundary. This method is very efficient to improve an initial shape. We give some numerical results.

Mathematics Subject Classification. 49J20, 49Q10, 65K10, 78A30.

Received: April 17, 2001. Revised: October 11, 2001.

Introduction

Let us consider a magnet Ω_0 which is located near a toothed wheel K. The magnetic field created by Ω_0 is of course different when it is a tooth of K which is faced to the magnet or when it is a hollow of the wheel. The first situation will be denoted in the following by the superscript T and the second one, by H. For example, $\mathbf{B}^T$ will be the magnetic vector induction when Ω_0 is faced to a tooth and $\mathbf{B}^H$ when it is faced to a hollow, see Figure 1. This kind of system is present in several technological devices (engine of a car, for example) and it is exactly the difference of the magnetic signals between the two situations which releases the desired action. In order to be very precise, the jump in the signal has to be the larger possible (with respect to some technological constraints). Therefore, an idea is to choose a shape of the magnet which allows to reach such a goal. The aim of this paper is to do a mathematical and numerical study of this problem.

In the sequel of this Introduction, we fix the notations, the constraints and we present a modelling of the problem as a tri-dimensional shape optimization (or optimum design) problem. In Section 2, we prove the existence of an optimum magnet in the natural class of uniformly Lipschitz open sets. In Section 3, we present the discretization and the numerical method we have followed to approximate an optimal domain. At last, Section 4 is devoted to numerical results and examples.

Let us first establish the set of equations which give the magnetic induction $\mathbf{B}$ for a *given configuration*. We will denote by Ω_0 the place occupied by the magnet and Γ_0 its boundary, K the toothed wheel, Ω_1 is the air surrounding the magnet and the wheel. We also introduce $\Omega = \overline{\Omega_0} \cup \Omega_1 = \mathbb{R}^3 \setminus K$ and denote by $\Gamma = \partial\Omega = \partial K$

Keywords and phrases. Shape optimization, optimum design, magnet, numerical examples.

* This work has been done thanks to a Grant of a firm from Besançon (France): Moving Magnet Technologies that we want to thank here.

[1] École des Mines de Nancy and Institut Elie Cartan, BP 239 54506 Vandœuvre-lès-Nancy, France.
e-mail: henrot@iecn.u-nancy.fr

[2] Centre de Recherche Valeo - Systèmes d'essuyage, Z.A. de l'Agiot, 78231 La Verrière, France.
e-mail: gregory.villemin@valeo.com

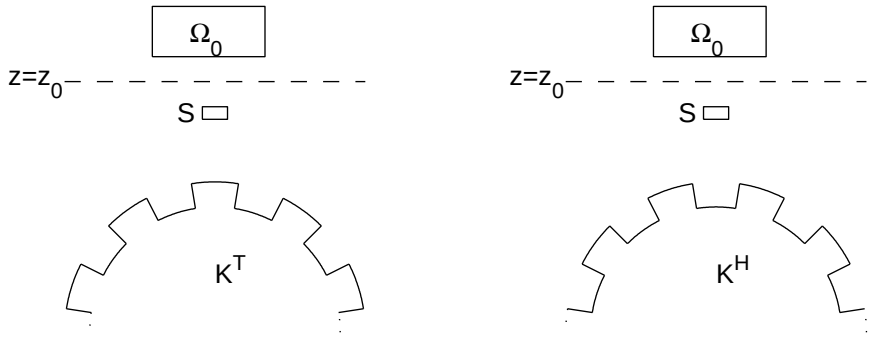

FIGURE 1. Magnet faced to a tooth (left), faced to a hollow (right).

its boundary. In the previous notations, we consider the sets $\Omega, \Omega_0, \Omega_1$ to be open connected domains in $\mathbb{R}^3$ and we assume their boundaries to be enough regular (at least Lipschitz). At last, we assume that the sound S is a compact regular set.

For all the quantities described below and the classical equations of magnetostatic, we refer *e.g.* to [5] or [7]. We will denote by $\mathbf{B}$ the magnetic induction vector, $\mathbf{H}$ the magnetic vector field and $\mathbf{M}$ the magnetization vector linked to the two previous quantities by the relation

$$\mathbf{B} = \mu_0(\mathbf{H} + \mathbf{M}) \tag{1}$$

(with $\mu_0 = 4\pi 10^{-7}$). Since we are in a magnetostatic context, Maxwell's equations can be written here in each medium separately as

$$\begin{cases} \operatorname{curl} \mathbf{H} = 0 \\ \operatorname{div} \mathbf{B} = 0. \end{cases} \tag{2}$$

Due to the first equation in (2), we are led to work with the scalar magnetic potential φ defined (up to a constant) such that $\mathbf{H} = -\nabla\varphi$.

Let us describe more precisely the equations in each media. We assume the magnet to be perfect and we choose its orientation in such a way that its magnetization is vertical. Therefore, if B_r is the retentivity of the magnet, we will set $M_0 = \frac{B_r}{\mu_0}$ and $\mathbf{M_0} = M_0 \overrightarrow{k}$. This yields that $\mathbf{M}$ is given in each media by

$$\mathbf{M} = (\mu_r - 1)\mathbf{H} + \mathbf{M_0} \tag{3}$$

where μ_r is the relative permeability of the media. Now,

- in the air $\mu_r = 1$ and $M_0 = 0$, so (1) and (3) yield $\mathbf{B} = \mu_0\mathbf{H} = -\mu_0\nabla\varphi$,
- in the magnet $\mu_r = 1$ and $M_0 \neq 0$, so (1) and (3) yield $\mathbf{B} = \mu_0(\mathbf{H} + \mathbf{M_0}) = \mu_0(\mathbf{M_0} - \nabla\varphi)$.

We express now the second equation in (2). In the air $\operatorname{div} \mathbf{B} = -\mu_0\Delta\varphi = 0$, while inside the magnet $\operatorname{div} \mathbf{B} = -\mu_0\Delta\varphi + \mu_0 \operatorname{div} \mathbf{M_0} = 0$. Now, since $\mathbf{M_0} = M_0 \overrightarrow{k}$ is constant its divergence vanishes and we still obtain $-\mu_0\Delta\varphi = 0$ in the magnet. In conclusion $\Delta\varphi = 0$ in $\Omega_0 \cup \Omega_1$.

It remains to express the magnetic induction field at the interface between the magnet and the air and to find the boundary conditions. The classical condition at the interface is the continuity of the magnetic flux (continuity of the normal component of $\mathbf{B}$). According to the expressions of $\mathbf{B}$, this condition gives

$$-\mu_0\nabla\varphi_{\Omega_1}.\mathbf{n} = -\mu_0\nabla\varphi_{\Omega_0}.\mathbf{n} + \mu_0\mathbf{M_0}.\mathbf{n} \tag{4}$$

where the subscript denotes the media where the potential φ has to be considered and $\mathbf{n}$ is the exterior normal vector to Γ_0. In other terms, the jump of the normal derivative of φ across the boundary of the magnet is equal to $\mathbf{M_0}.\mathbf{n}$. It means that, if we consider φ to be globally defined in the whole domain Ω, its Laplacian is a measure supported by Γ_0 of intensity $\mathbf{M_0}.\mathbf{n}$:

$$-\Delta\varphi = L_0 \quad \text{in } \Omega \tag{5}$$

where L_0 is the linear form defined on the weighted Sobolev space $W_0^1(\Omega)$ (for a precise definition of this space which corresponds to the classical Sobolev space H_0^1 with the weight $(1+r^2)^{-1/2}$, we refer to [5] XI B, Def. 2) by

$$\langle L_0, w\rangle := \int_{\Gamma_0} \mathbf{M_0}.\mathbf{n}\, w \,\mathrm{d}\sigma. \tag{6}$$

This linear form is well defined and continuous on $W_0^1(\Omega)$ by continuity of the trace operator. Let us now establish the boundary conditions: since the wheel is an equipotential, and according to the fact that φ is defined up to a constant, we can fix $\varphi = 0$ on $\partial\Omega$. At last, since there is no current at infinity, we have $\varphi(X) \to 0$ when $|X| \to +\infty$.

To sum up, we have obtained the following set of equations which define φ in an unique way

$$\left\{\begin{array}{rcll} -\Delta\varphi &=& L_0 & \text{in } \Omega \\ \varphi &=& 0 & \text{on } \partial\Omega \\ \varphi(X) &\to& 0 & \text{when } |X| \to +\infty. \end{array}\right. \tag{7}$$

The problem (7) is well posed (see *e.g.* [5]). Introducing the fundamental solution of $-\Delta u_\infty = L_0$ in $\mathbb{R}^3$ defined by

$$u_\infty(X) = \frac{1}{4\pi}\int_{\Gamma_0} \frac{\mathbf{M_0}.\mathbf{n}}{|X-Y|}\,\mathrm{d}\sigma_Y \tag{8}$$

we can decompose φ as

$$\varphi = u_\infty - v \tag{9}$$

where v is the harmonic function, taking the value u_∞ on Γ and vanishing at infinity. In other words, we can choose an integral formulation to solve (7). It consists in writing φ as (simple layer potential)

$$\varphi(X) = \frac{1}{4\pi}\int_{\Gamma_0} \frac{\mathbf{M_0}.\mathbf{n}}{|X-Y|}\,\mathrm{d}\sigma_Y - \frac{1}{4\pi}\int_{\Gamma} \frac{\alpha(Z)}{|X-Z|}\,\mathrm{d}\sigma_Z \tag{10}$$

where the function α is obtained by solving the 1st kind Fredholm integral equation (expressing the boundary condition on Γ):

$$\forall X \in \Gamma : \quad \int_{\Gamma_0} \frac{\mathbf{M_0}.\mathbf{n}}{|X-Y|}\,\mathrm{d}\sigma_Y = \int_{\Gamma} \frac{\alpha(Z)}{|X-Z|}\,\mathrm{d}\sigma_Z. \tag{11}$$

We must now describe the criterion we want to optimize. Physically, the magnetic field is measured by a sound S located between the magnet and the wheel, see Figure 1. We recall that we have to consider two different situations. If ω is a given magnet, we will denote by φ_ω^T (or simply φ^T if there is no misunderstanding) the magnetic potential when ω is faced to a tooth and φ_ω^H (or simply φ^H) when it is faced to a hollow. Since we

want to find some magnet ω such that the gap between the two situations is maximum, we choose to introduce the following functional:

$$J(\omega) = \frac{1}{2} \int_S |\nabla \varphi_\omega^T(X)|^2 - |\nabla \varphi_\omega^H(X)|^2 \, \mathrm{d}X. \tag{12}$$

Of course, we need to put some constraints on the class of admissible magnets. For obvious technical reasons, we fix a maximum value V_0 for the volume. In the paper, we will denote by $|\omega|$ the volume of the set ω and by $|\partial\omega|$ its surface area. Moreover, in order to avoid that the magnet comes in contact with the sound or the wheel, we will fix a lower plane $z = z_0$ above which the magnet must hold, see Figure 1. In the numerical approach, the volume constraint will be treated by penalization: we will substract to the functional J a term like $r\left[(|\omega| - V_0)^+\right]^2$ (where $(A)^+$ denotes, as usual, the positive part of the number A) with a large parameter r of penalization. Therefore the functional we really maximize is

$$J_r(\omega) := \frac{1}{2} \int_S |\nabla \varphi_\omega^T(X)|^2 - |\nabla \varphi_\omega^H(X)|^2 \, \mathrm{d}X - r\left[(|\omega| - V_0)^+\right]^2 . \tag{13}$$

The other constraint will be treated by projection.

The aim of this work is to look for a domain Ω satisfying the constraints and which maximizes the functional J given in (12).

1. An existence result

1.1. Introduction

In this section, we will prove existence of a maximizer for the functional J in the natural class of uniformly Lipschitz open sets in $\mathbb{R}^3$. This class can also be described as sets with the ε-cone property, and it has been introduced by Chenais in her important work, see [3, 4]. In Section 1.2, we recall the definition of the ε-cone property. We prove, in particular, that sets in this class with bounded volume have also an uniformly bounded area. In Section 1.3, we prove that the functional J is estimated from above in this class. In the sequel, our approach is a classical one: we work with a maximizing sequence and Hausdorff convergence. The difficulty in our case is that the sets we consider are *a priori* unbounded and could have components which go to infinity. Now, if we want to use the compactness property of the Hausdorff convergence, we need to work with domains which are all contained in some fixed ball. That is why we will distinguish, in the proof of existence, components of the maximizing sequence which go to infinity of those which stay at finite distance of the wheel (see Sect. 1.5).

Here the result of continuity with respect to the domain that we need is not too difficult to get, because domain variation is only expressed in the linear form in the right hand side of the equation. Moreover, since the functional J has to be calculated on a region S where all the functions are harmonic, we can use the powerful properties of convergence of sequence of harmonic functions.

1.2. The class of admissible sets

We recall here the definition of the ε-cone property (see [1, 3, 4, 8]).

Definition 1.1. Let Y a point in $\mathbb{R}^3$, ξ a unit vector and ε a positive number, $\varepsilon < \pi/2$. We introduce the cone $C(Y, \xi, \varepsilon)$ as the set defined by:

$$C(Y, \xi, \varepsilon) = \{Z \in \mathbb{R}^3,\ (Z - Y, \xi) \geq |Z - Y| \cos(\varepsilon) \text{ and } 0 < |Z - Y| < \varepsilon\}$$

(where $(.,.)$ denotes the usual scalar product in $\mathbb{R}^3$ and $|.|$ the associated Euclidean norm).

We will say that an open set ω has the ε-cone property (with $\varepsilon > 0$ is fixed), if

$$\forall X \in \partial\omega,\ \exists \xi_X \text{a unit vector such that } \forall Y \in \overline{\omega} \cap B(X,\varepsilon)\ C(Y,\xi_X,\varepsilon) \subset \omega. \tag{14}$$

Indeed, the ε-cone property is equivalent for a set to have a boundary which is uniformly Lipschitz. That means that, locally, $\partial\omega$ can be written as a graph of a Lipschitzian function, the Lipschitz constant L being the same for all boundary points. More precisely, we will use later on the following property:
$\forall X \in \partial\omega$, there exist reference axis centered at X with a third (vertical) vector ξ_X and a function ψ Lipschitzian, with a Lipschitz constant $L = \cot\varepsilon/2$ such that, if we denote by C_ε the cylinder which have for base the disk D_ε of radius $\varepsilon\tan\varepsilon$ and for height $[-\varepsilon,\varepsilon]$, we have

$$\begin{cases} \partial\omega \cap C_\varepsilon = \{(x,y,z) \in C_\varepsilon\ /z = \psi(x,y) \quad (x,y) \in D_\varepsilon\} \\ \omega \cap C_\varepsilon = \{(x,y,z) \in C_\varepsilon\ /z > \psi(x,y) \quad (x,y) \in D_\varepsilon\}. \end{cases} \tag{15}$$

This property is well known, one can find a proof *e.g.* in [4] or [8].

Let us now precise the class of admissible sets for our maximization problem. We include in this definition the two constraints presented above:

Definition 1.2. Let us consider a fixed positive number ε, we will denote by $\mathcal{C} = \mathcal{C}(\varepsilon, V_0, z_0)$ the class of admissible sets defined by:

$$\mathcal{C} = \left\{\omega \subset \mathbb{R}^3\ ,\ \omega \text{ has the } \varepsilon\text{-cone property }, |\omega| \leq V_0,\ \omega \text{ is located above the plane } z = z_0\right\}.$$

Since the linear form in the right-hand side of (7) is calculated using a boundary integral over $\partial\omega$, we will need the uniform boundedness of the area for the sets in the class $\mathcal{C}$:

Proposition 1.3. *There exists a constant C depending only on ε and V_0 such that*

$$\forall \omega \in \mathcal{C} \quad |\partial\omega| \leq C. \tag{16}$$

Proof. Let us introduce $\tilde{\varepsilon} = \min(\varepsilon, \varepsilon\tan\varepsilon)$. Since ω has the ε-cone property, it has also the $\tilde{\varepsilon}$-cone property. Let us recover $\mathbb{R}^3$ with cubes (with disjoints interiors) of side length $\frac{\tilde{\varepsilon}}{\sqrt{3}}$. We denote by $\mathcal{N}$ the collection of those cubes which meet $\partial\omega$ and N the cardinal of $\mathcal{N}$ (N could be *a priori* infinite, but the proof will show that it is uniformly bounded for all sets in the class $\mathcal{C}$).

Let K_1 be a cube in $\mathcal{N}$, $X_1 \in K_1 \cap \partial\omega$. and C_1 the cone $C(X_1, \xi_{X_1}, \tilde{\varepsilon})$ which is contained in ω by $\tilde{\varepsilon}$-cone property. Since the diameter of this cone is $\tilde{\varepsilon}$ and the diameter of an elementary cube is also $\tilde{\varepsilon}$, by construction C_1 can meet at most 27 cubes of the covering. Now the alternative is the following:

- either ω is contained in the union of these 27 cones and we stop,
- or it is not the case and we do again the same process by choosing a new cube K_2, not in the previous list, a new point X_2 and a new cone C_2 disjoint from C_1.

Since the volume V_0 of ω is greater or equal to the sum of the (fixed) volume of each cones, this process has to stop. This shows that the number N of cubes which meet ω is bounded by $N \leq \frac{V_0}{27|C_\varepsilon|}$ where $|C_\varepsilon|$ is the volume of a cone.

Now, since

$$|\partial\omega| = \sum_{K\in\mathcal{N}} |\partial\omega \cap K| \leq N \max_{K\in\mathcal{N}} |\partial\omega \cap K|,$$

it is enough to estimate the area of $\partial\omega$ on each elementary cube. But, if $X \in K \cap \partial\omega$, we have, according to the respective dimensions

$$\partial\omega \cap K \subset \partial\omega \cap B(X,\tilde{\varepsilon}).$$

So, using (15), we have

$$|\partial\omega \cap B(X,\tilde{\varepsilon})| = \iint_{D_\varepsilon} \sqrt{1+\left(\frac{\partial\psi}{\partial x}\right)^2+\left(\frac{\partial\psi}{\partial y}\right)^2}\,\mathrm{d}x\mathrm{d}y \leq \sqrt{1+2L^2}\pi\tilde{\varepsilon}^2$$

what implies the desired result. □

Remark 1.4.

1. Because of the volume constraint, it is easy to verify that the number of cubes which recover a set ω in $\mathcal{C}$ is also uniformly bounded by a constant N_1 depending only on ε and V_0.
2. The diameter of sets in the class $\mathcal{C}$ is not uniformly bounded: we can imagine two balls of fixed radius going away each other. On the other hand, it is easy to prove, using the covering, that the diameter of each connected component of ω must be uniformly bounded.
3. Because of the ε-cone property, the volume of each connected component of ω is bounded from below (by the volume of an elementary cone), therefore the number of connected component of ω is uniformly bounded by an integer that we will denote by N_0.

1.3. **Estimation of the functional *J***

Since we are interested in the maximization of the functional J, we will first prove that it is estimated from above:

Proposition 1.5. *There exists a constant C', depending only on the data $\varepsilon, V_0, z_0, M_0$ such that*

$$\forall\omega \in \mathcal{C} \quad J(\omega) \leq C'.$$

Proof. Let ω be a fixed set in the class $\mathcal{C}$, we denote by Γ_0 its boundary and Ω the complementary of the wheel (Γ being the boundary of Ω). We use here the notations of section 1 (see (9)). By maximum principle and (8), we have

$$\sup_{\Omega}|v| = \sup_{\Gamma}|u_\infty| \leq \frac{1}{4\pi}\frac{|M_0||\partial\omega|}{d(\Gamma_0,\Gamma)}$$

where $d(\Gamma_0,\Gamma) := \inf\{|X_0 - X_1|, X_0 \in \Gamma_0, X_1 \in \Gamma\}$ denotes the distance between Γ_0 and Γ which is bounded from below by some positive distance δ_1.

Now, let us fix an open neighbourhood $\hat{S}$ of S which does not intersect Ω_0 and K. In the same way, we have

$$\sup_{\hat{S}}|u_\infty| \leq \frac{1}{4\pi}\frac{|M_0||\partial\omega|}{d(\Gamma_0,\hat{S})}$$

with $d(\Gamma_0,\hat{S})$ bounded from below by some positive distance δ_2.

This yields the following estimate for φ on $\hat{S}$:

$$\forall X \in \hat{S} \quad |\varphi(X)| \leq \frac{|M_0||\partial\omega|}{4\pi}\left(\frac{1}{d(\Gamma_0,\Gamma)}+\frac{1}{d(\Gamma_0,\hat{S})}\right). \tag{17}$$

In (17), the right-hand side can be bounded independently of ω, thanks to Proposition 1.3 and the previous remarks.

We deduce now from (17) and from usual representation formulae for harmonic functions, an uniform estimate for $|\nabla\varphi|^2$ on S, and Proposition 1.5 follows. □

1.4. **Continuity with respect to the domain**

As it is usual in many shape optimization problems, we choose to work with the Hausdorff distance of open sets. Let us recall its definition:

Definition 1.6. Let K_1 and K_2 be compact subsets in $\mathbb{R}^3$, we define their Hausdorff distance by

$$d_H(K_1, K_2) := \sup_{X \in \mathbb{R}^3} |d(X, K_1) - d(X, K_2)|.$$

If ω_1 and ω_2 are two bounded open sets in $\mathbb{R}^3$, we fix a ball B containing both and we set

$$d_H(\omega_1, \omega_2) := d_H(B \setminus \omega_1, B \setminus \omega_2).$$

(it is easy to verify that this definition doesnot depend on the choice of the ball B containing the two open sets).

We will say that a sequence ω_n Hausdorff-converges to ω if $d_H(\omega_n, \omega) \to 0$.

Let us recall some classical properties of the Hausdorff convergence, for the proofs we refer to [8, 11], or [3].

Proposition 1.7.

(i) *(compactness) Let B be a fixed ball and ω_n a sequence of open sets contained in B. Then, there exists a subsequence ω_{n_k} and an open set $\omega \subset B$ such that ω_{n_k} Hausdorff-converges to ω.*

(ii) *Let ω_n be a sequence of open sets which Hausdorff-converges to ω and $X \in \partial\omega$. Then, there exists a sequence of points $X_n \in \partial\omega_n$ which converges to X.*

(iii) *Let ω_n be a sequence of open sets which have the ε-cone property (for some fixed $\varepsilon > 0$). We assume that ω_n Hausdorff-converges to ω. Then, ω has the ε-cone property. Moreover, χ_{ω_n} (the characteristic function of ω_n) converges in $L^1_{loc}(\mathbb{R}^3)$ to χ_ω.*

The property (iii) shows, in particular, that the class $\mathcal{C}$ defined above (see Def. 1.2) is closed for the Hausdorff-convergence since the two constraints will also pass to the limit:

- $|\omega_n| = \int_B \chi_{\omega_n} \to \int_B \chi_\omega = |\omega|$
- $\omega_n \subset \{z \geq z_0\} \quad \Longrightarrow \quad \omega \subset \{z \geq z_0\}$ (since Hausdorff convergence preserves the inclusion).

For every open set ω in the class $\mathcal{C}$, we will denote by L_ω the linear form defined on $W^1_0(\Omega)$ by (6). We will also denote by φ_ω the solution of (7), with right-hand side L_ω. In the following result, we consider two kinds of situations: a sequence of domains ω_n which goes to infinity and a sequence of domains which Hausdorff-converges.

Theorem 1.8.

1. *If ω_n is a sequence of sets in the class $\mathcal{C}$ which goes to infinity (in the sense that $d(0, \omega_n) \to +\infty$), then φ_{ω_n} converges uniformly to 0, as all its derivatives, on S.*
2. *If ω_n is a sequence of sets in the class $\mathcal{C}$ which Hausdorff-converges to ω, then φ_{ω_n} converges uniformly to φ_ω, and all the derivatives of φ_{ω_n} converges uniformly to the corresponding derivatives of φ_ω, on S.*

Proof. The first case follows immediately from formula (17). Indeed, if ω_n goes to infinity, it is the same for each distance $d(\Gamma_{0,n}, \Gamma)$ and $d(\Gamma_{0,n}, \hat{S})$ and the result follows for φ_{ω_n} according to (17) since $|\partial\omega_n|$ is uniformly bounded. Now, the result is also true for the derivatives due to classical properties of sequences of harmonic functions (Harnack's inequalities).

The second case is a little bit more complicated. We write, as in (9), $\varphi_{\omega_n} = u_\infty^{\omega_n} - v^{\omega_n}$ where

$$u_\infty^{\omega_n}(X) = \frac{1}{4\pi} \int_{\partial\omega_n} \frac{\mathbf{M_0}.\mathbf{n}}{|X - Y|} \, \mathrm{d}\sigma_Y$$

and v^{ω_n} is the harmonic function, taking the value $u_\infty^{\omega_n}$ on Γ and vanishing at infinity (and similarly replacing ω_n by ω).

Let us first prove that $u_\infty^{\omega_n}$ converge uniformly to u_∞^{ω} on every compact subset K of $(\overline{\omega})^c$ (according to classical properties of Hausdorff convergence, such a compact is included in $(\overline{\omega_n})^c$ for n large enough). Let $\hat{X}$ be fixed on K, we denote by $w(Y)$ the function $\dfrac{1}{|\hat{X}-Y|}$. We begin to work locally. Let $X \in \partial\omega$ and ξ_X the direction of the cone associated to X. According to Proposition 1.7, there exists a sequence of points X_n, each lying on the boundary of ω_n, which converge to X. Moreover, we know (*cf.* [8] or [3]) that we are always able to choose the sequence of associated cone directions ξ_{X_n} in order that they converge to ξ_X. Therefore, for n large enough, the boundary of ω_n in a neighbourhood of X_n can be written as a graph of a function ψ_n $(L+1)$-Lipschitzian in some local coordinate system $\mathcal{R}_X$ associated to the point X with vertical vector ξ_X (see (15)). The functions ψ_n being uniformly Lipschitzian, by Ascoli's Theorem we can extract a subsequence, still denoted by ψ_n, which converges uniformly to a Lipschitzian function ψ. It is classical then that ψ defines locally the boundary of ω in a neighbourhood of X. Since ψ is the only accumulation point of the sequence ψ_n, the whole sequence converges to ψ.

Let us denote by γ_n (resp. γ), the intersection of $\partial\omega_n$ (resp. $\partial\omega$) with the cylinder C_ε, neighbourhood of X in which the parametrizations defined by ψ_n and ψ are valid. Denoting by $M_0 = (A, B, C)^T$, we have in $\mathcal{R}_X$:

$$\int_{\gamma_n} w(\sigma)\, M_0.n(\sigma)\, \mathrm{d}\sigma = \int_{D_\varepsilon} w(x, y, \psi_n(x, y))(-A\frac{\partial \psi_n}{\partial x} - B\frac{\partial \psi_n}{\partial y} + C)\, \mathrm{d}x\mathrm{d}y$$

and similarly for $\int_\gamma w(\sigma)\, M_0.n(\sigma)\, \mathrm{d}\sigma$.

On one hand, $w(x, y, \psi_n(x, y))$ converge uniformly to $w(x, y, \psi(x, y))$ on D_ε according to the beginning of the proof. On the other hand, ψ_n converges uniformly to ψ, $\dfrac{\partial \psi_n}{\partial x}$ and $\dfrac{\partial \psi_n}{\partial y}$ converge in the sense of distributions to $\dfrac{\partial \psi}{\partial x}$ and $\dfrac{\partial \psi}{\partial y}$ respectively. But, since $\dfrac{\partial \psi_n}{\partial x}$ and $\dfrac{\partial \psi_n}{\partial y}$ are bounded in L^∞ (because of the uniform Lipschitz property of the functions ψ_n), the convergence takes place indeed in L^∞ weak-$*$. Therefore the duality pair $\langle w(x, y, \psi_n(x, y)), -A\frac{\partial \psi_n}{\partial x} - B\frac{\partial \psi_n}{\partial y} + C\rangle$ converge to $\langle w(x, y, \psi(x, y)), -A\frac{\partial \psi}{\partial x} - B\frac{\partial \psi}{\partial y} + C\rangle$ what proves the result locally. We conclude thanks to a finite covering of $\partial\omega$ by neighbourhoods of the kind C_ε and by using a corresponding partition of the unity. We have proved indeed that $u_\infty^{\omega_n}$ simply converge to u_∞^{ω}, but since it is a bounded sequence of harmonic functions, we have in fact uniform convergence on every compact.

Now, by maximum principle, the convergence of $u_\infty^{\omega_n}$ to u_∞^{ω} implies convergence of v^{ω_n} to v^{ω} on every compact subset of $(\overline{\omega})^c$.

So, φ_{ω_n} converge to φ_ω on every compact subset of $(\overline{\omega})^c$. By Harnack inequalities, the convergence takes place also for the derivatives of φ_{ω_n}. □

1.5. **The existence result**

We can now claim the main result of this section:

Theorem 1.9. *The functional J defined in (12) achieves its maximum on the class $\mathcal{C}$.*

Proof. Let us consider a maximizing sequence ω_n. According to the Remark 1.4 above, each open set ω_n has at most N_0 connected components. We can thus decompose it as

$$\omega_n = \omega_n^1 \cup \omega_n^2 \cup \ldots \cup \omega_n^{N_0} \tag{18}$$

where in the decomposition (18), some connected components could be empty and all the connected components are disjoints. By the linearity of the problem, we can write in a similar way

$$L_{\omega_n} = L_{\omega_n^1} + L_{\omega_n^2} + \ldots + L_{\omega_n^{N_0}} \tag{19}$$

where, by convention $L_\emptyset = 0$. In the previous decomposition, we use the fact that the open set ω being Lipschitzian, two different connected components cannot have a common boundary part (ω_n has to be on one side of its boundary). Still by a linearity argument, we deduce from (19), the corresponding decomposition for φ_{ω_n}:

$$\varphi_{\omega_n} = \varphi_{\omega_n^1} + \varphi_{\omega_n^2} + \ldots + \varphi_{\omega_n^{N_0}} \tag{20}$$

(with $\varphi_\emptyset = 0$). We are now working with each connected component separately. Let us study the sequence ω_n^1. There are two possibilities:

- either, there exists a subsequence $\omega_{n_k}^1$ which stay confined in a ball. In this case, we can extract a subsequence which converges in the Hausdorff sense to an open set ω^1 (which has the ε-cone property).
- or the whole sequence ω_n^1 goes to infinity, and we set $\omega^1 = \emptyset$.

By doing the same for each connected component, we are able, after a finite number of such operations, to construct a subsequence ω_{n_k} of the maximizing sequence ω_n and an open set $\omega \in \mathcal{C}$ defined by

$$\omega = \omega^1 \cup \omega^2 \cup \ldots \cup \omega^{N_0}.$$

According to Theorem 1.8 and (20) we have that $\varphi_{\omega_{n_k}}$ converge in the harmonic sense to φ_ω. Therefore $J(\omega_{n_k})$ converge to $J(\omega)$ which yields the desired result. □

Remark 1.10. It is clear that the empty set could not be a maximiser of J. Indeed, we are always able to exhibit an open set ω in the class $\mathcal{C}$ such that $J(\omega) > 0 = J(\emptyset)$ (see Sect. 3). Therefore, the above existence result yields a global maximum in the class $\mathcal{C}$. Nevertheless, since our numerical algorithm, described in the next section, does not change the topology of the initial guess, we cannot see if pieces of a minimizing sequence would like to go to infinity. Moreover, it could also converge to a local minimizer, see also final comments.

2. Discretization of the problem

2.1. Introduction

In this section, we want to explain the way we deform the successive magnets in order to increase the value of the functional J. We follow the same idea as in [9, 10]. The method consists in constructing a sequence $(\Gamma_0^k, \varphi^k, V^k)_{k=1,\ldots,n}$ where

- Γ_0^k is a triangular mesh representing the magnet at the k-th iteration. Each triangle T_l is parametrized by a reference triangle $\hat{T}$ of coordinates ξ and η. Therefore, if $X^{l,1}, X^{l,2}, X^{l,3}$ are the vertices of the triangle T^l, each point of the triangle can be represented by

$$X = X(\xi, \eta) = \sum_{i=1}^{3} X^{l,i} N_i(\xi, \eta)$$

where

$$N_1(\xi, \eta) = 1 - \xi - \eta, \quad N_2(\xi, \eta) = \xi, \quad N_3(\xi, \eta) = \eta.$$

In the sequel, we will denote by X_ξ and X_η the derivative of X with respect to ξ and η, that is to say, with the previous formulae:

$$X_\xi = X^{l,2} - X^{l,1} \qquad X_\eta = X^{l,3} - X^{l,1}.$$

- φ_k^T and φ_k^H denote the magnetic scalar potentials (in each situation) created by the magnet whose boundary is Γ_0^k. Each are solutions of a problem like (7).

- V^k denotes the vector field which gives the direction of the displacement at each node of Γ_0^k. More precisely, if the nodes are denoted by $(X_i^k)_{i=1..M}$, for each node X_i^k, we choose the direction V_i^k as the weighted average of the exterior normal vectors to triangles having X_i^k as a vertex.

Now, we have to decide how much we will deform the magnet Γ_0^k at each vertices in the direction V_i^k. So, we introduce the unknowns $(u_i)_{i=1..M}$ which are the **intensity** of the deformation of the nodes X_i^k in the direction V_i^k. In other terms, we have to find a vector in $\mathbb{R}^M$: $U = (u_i)_{i=1..M}$ which maximizes (at least locally) the functional $J(\Gamma_0^U) := J^k(U)$ where Γ_0^U is the boundary of the magnet whose nodes are the points $X_i^U := X_i^k + u_i V_i^k$.

We simply improve the functional $J^k(U)$ with the help of a quasi-Newton B.F.G.S. method (see *e.g.* [2] or [6]). At each iteration we must compute the gradient with respect to U of the functional J^k at $U = 0$.

2.2. Computation of the discretized gradient

We give first the value of the gradient for the continuous problem. It helps to well understand the formula for the discretized problem. We use here the classical tool of the derivative with respect to the domain. See references below.

Proposition 2.1. *Let φ the solution of (7), and j the functional defined by*

$$j(\Omega_0) = \int_S |\nabla\varphi(X)|^2 \, \mathrm{d}X. \tag{21}$$

Assume that Ω_0 is of class C^2, then the derivative of j at Ω_0 with respect to a deformation of the boundary induced by the vector field V is given by

$$dj(\Omega_0, V) = -\int_{\Gamma_0} M_0.\nabla_{\Gamma_0}(V.\mathbf{n})p \, \mathrm{d}\sigma + \int_{\Gamma_0} M_0.\mathbf{n}pH(V.\mathbf{n}) \, \mathrm{d}\sigma + \int_{\Gamma_0} \frac{\partial p}{\partial n} M_0.\mathbf{n}(V.\mathbf{n}) \, \mathrm{d}\sigma \tag{22}$$

where ∇_{Γ_0} denotes the tangential gradient on the boundary Γ_0, H is the mean curvature of Γ_0 and p is the adjoint state, solution of the following problem:

$$\left\{ \begin{array}{rcll} -\Delta p & = & L_S & \text{in } \Omega \\ p & = & 0 & \text{on } \partial\Omega \\ p(X) & \to & 0 & \text{when } |X| \to +\infty \end{array} \right. \tag{23}$$

where L_S is the linear form defined on $W_0^1(\Omega)$ by

$$\langle L_S, w\rangle := \langle -\nabla\chi_S.\nabla\varphi, w\rangle = \sum_{i=1}^{3} \int_S \frac{\partial}{\partial x_i}\left(\frac{\partial\varphi}{\partial x_i} w\right) \mathrm{d}\sigma_S. \tag{24}$$

The proof follows straigthforward calculations and classical formulae given in the papers of Simon [12, 13] or the books of Sokolowski-Zolesio [14] or Henrot-Pierre [8]. We omit it here.

We can easily deduce, from the previous formula (22), the expression of the derivative, with respect to the domain, of the functional J defined in (12). We can imagine that this formula is not very suitable from a computational point of view, due to terms involving the mean curvature or the tangential gradient. That is the reason why we have chosen to compute directly the gradient of the discretized functional rather than discretizing the continuous gradient.

We want to compute the gradient of the functional j defined in (21) with respect to the variable u_i at $u = 0$. It means that we deform the initial magnet by moving only the ith node of some distance h_i, we set $\Omega_0^{h_i}$ the new magnet, and we have to calculate

$$\lim_{h_i \to 0} \frac{j(\Omega_0^{h_i}) - j(\Omega_0)}{h_i}.$$

The computation involves the function φ_i solution of (7) with a right-hand side L_0^i defined by (6) on the magnet $\Omega_0^{h_i}$. First, we want to compute the limit, when $h_i \to 0$ of the function $w^{h_i} := \dfrac{\varphi_i - \varphi}{h_i}$. Let us decompose this quotient as (see (9))

$$\frac{\varphi_i - \varphi}{h_i} = \frac{u_\infty^i - u_\infty}{h_i} + \frac{v_i - v}{h_i}$$

with

$$u_\infty^i(X) = \frac{1}{4\pi} \int_{\partial\Omega_0^{h_i}} \frac{\mathbf{M_0}.\mathbf{n}}{|X-Y|}\, \mathrm{d}\sigma_Y$$

and v_i is the harmonic function, taking the value u_∞^i on Γ and vanishing at infinity (and the same for Ω_0).

Lemma 2.2. *The sequence of functions* $\dfrac{u_\infty^i - u_\infty}{h_i}$ *converge (uniformly on every compact subset of the exterior of* Ω_0*), when* $h_i \to 0$*, to the function* U_i *defined by*

$$U_i(X) = \left\langle L_i', \frac{1}{|X-Y|} \right\rangle \tag{25}$$

where L_i' *is the linear form defined by*

$$\begin{aligned} \langle L_i', w\rangle := {} & \textstyle\sum_j \int_{\hat T} \{\mathbf{M_0}.\mathbf{Q_j}\, w + (1-\xi-\eta)\mathbf{M_0}.\mathbf{n_j}\, \nabla w.V_i\}\, |X_\xi \wedge X_\eta|\, \mathrm{d}\xi\, \mathrm{d}\eta \\ & + \textstyle\sum_j \int_{\hat T} \{\mathbf{M_0}.\mathbf{n_j}\}\ w\mathbf{n_j}.(V_i \wedge (X^{j_1} - X^{j_2}))\, \mathrm{d}\xi\, \mathrm{d}\eta \end{aligned} \tag{26}$$

where $\hat T$ *is the reference triangle and* $\mathbf{Q_j}$ *is the vector defined by*

$$\mathbf{Q_j} = \frac{2(V_i.\mathbf{n_j})(\mathbf{n_j} \wedge (X^{j_1} - X^{j_2})}{|T_j|}$$

the above sum is done on all the triangles T_j *containing* X^i *as a vertex,* X^{j_1} *and* X^{j_2} *being the two other vertices of* T_j*,* $\mathbf{n_j}$ *its normal vector and* $|T_j|$ *the area of* T_j*. The vector* V_i *is defined in Section 2.1; it is the weighted average of the normal vectors* $\mathbf{n_j}$*.*

Proof. Let X be fixed in the proof and let us denote by $w(Y)$ the function $Y \mapsto \frac{1}{|X-Y|}$. By definition, we have

$$R(h_i) := \frac{u_\infty^i(X) - u_\infty(X)}{h_i} = \frac{1}{h_i}\left[\int_{\Gamma_0^i} \mathbf{M_0}.\mathbf{n_{h_i}} w\, \mathrm{d}\sigma_i - \int_{\Gamma_0} \mathbf{M_0}.\mathbf{n} w\, \mathrm{d}\sigma\right] \tag{27}$$

where Γ_0^i is the boundary of the deformed magnet $\Omega_0^{h_i}$. It is clear on the previous formula (27) that the only contribution will come from the triangles which contain the ith node X^i. So let us introduce ΣT^i the set of triangles containing X^i **before** the deformation and ΣT^{h_i} the set of triangles containing X^i **after** the deformation of intensity h_i. Therefore,

$$R(h_i) = \frac{1}{h_i}\left[\int_{\Sigma T^{h_i}} \mathbf{M_0}.\mathbf{n_{h_i}} w\, \mathrm{d}\sigma_i - \int_{\Sigma T^i} \mathbf{M_0}.\mathbf{n} w\, \mathrm{d}\sigma\right]. \tag{28}$$

Let us consider one triangle, say T_j in ΣT^i whose vertices are X^i, X^{j_1}, X^{j_2}. The deformed triangle $T_j^{h_i}$ has for vertices $X^i + h_i V_i, X^{j_1}, X^{j_2}$. Coming back to the reference triangle yields:

$$\int_{T_j^{h_i}} \mathbf{M_0}.\mathbf{n_{j,h_i}} w\, \mathrm{d}\sigma_i = \int_{\hat T} \mathbf{M_0}.\mathbf{n_{j,h_i}} w[(1-\xi-\eta)(X^i + h_i V_i) + \xi X^{j_1} + \eta X^{j_2}] \left| X_\xi^{j,h_i} \wedge X_\eta^{j,h_i} \right| \mathrm{d}\xi\, \mathrm{d}\eta.$$

Now using the elementary expansions:

- $\mathbf{n_{j,h_i}} = \mathbf{n_j} + h_i \frac{(V_i.\mathbf{n_j})\left(\mathbf{n_j} \wedge (X^{j_1} - X^{j_2})\right)}{2|T_j|} + o(h_i)$,
- $w[(1-\xi-\eta)(X^i + h_i V_i) + \xi X^{j_1} + \eta X^{j_2}] = w[(1-\xi-\eta)X^i + \xi X^{j_1} + \eta X^{j_2}] + (1-\xi-\eta)h_i \nabla w.V_i + o(h_i)$,
- $\left| X_\xi^{j,h_i} \wedge X_\eta^{j,h_i} \right| = \left| (X^{j_1} - X^i - h_i V_i) \wedge (X^{j_2} - X^i - h_i V_i) \right| = \left| X_\xi^j \wedge X_\eta^j \right| + h_i \left(V_i \wedge (X^{j_1} - X^{j_2}) \right) .\mathbf{n_j} + o(h_i)$

and adding on the different triangles containing X^i gives the desired result thanks to straightforward calculations. Once again, we use the fact that, for a sequence of bounded harmonic functions, simple convergence implies uniform convergence on every compact sets. □

Now, differentiation of the integral formula which defines j gives:

Proposition 2.3. *The derivative of the functional j defined in (21) with respect to the variable u_i at $u = 0$ is given by*

$$\frac{\partial j}{\partial u_i}_{|u=0} = 2 \int_S \nabla\varphi.\nabla w_i \, \mathrm{d}X \tag{29}$$

where φ is the solution of (7) and w_i is defined by

$$w_i = U_i - \Phi_i \tag{30}$$

where U_i is defined in (25), (26) and Φ_i is the harmonic function taking the value U_i on Γ and vanishing at infinity.

2.3. **The adjoint problem**

As it is classical in optimal control problems, it is more convenient to express the previous derivative thanks to the use of *an adjoint state*. We will denote by χ_S the characteristic function of the regular set S. Therefore, $\nabla\chi_S$ is a (positive) measure supported by the boundary of S. In particular, we can consider the following linear form $L_S := -\nabla\chi_S.\nabla\varphi$ which is well defined on the weighted Sobolev space $W_0^1(\Omega)$ by

$$\langle L_S, w\rangle := \langle -\nabla\chi_S.\nabla\varphi, w\rangle = \sum_{i=1}^{3} \int_S \frac{\partial}{\partial x_i}\left(\frac{\partial\varphi}{\partial x_i}\, w\right) \mathrm{d}\sigma_S \tag{31}$$

(notice that φ is C^∞ inside Ω so, in particular, on S). Let us now introduce the function p solution of the following boundary value problem:

$$\left\{ \begin{array}{rcll} -\Delta p &=& L_S & \text{in } \Omega \\ p &=& 0 & \text{on } \partial\Omega \\ p(X) &\to& 0 & \text{when } |X| \to +\infty \, . \end{array} \right. \tag{32}$$

We can easily prove thanks to the Green formula (note that p is C^∞ on Ω_0, so $\langle L_i', p\rangle$ is well defined):

Proposition 2.4. $\dfrac{\partial j}{\partial u_i}_{|u=0} = \langle L_i', p\rangle$ *with L_i' given in (26) and p solution of (32).*

Of course, the interest of such a formula is to prevent computing each function w_i: it is sufficient to solve only the direct and the adjoint problem to get the derivative of the functional into consideration. The expression of the whole derivative follows immediately from the previous formula by considering the two situations (faced with a tooth or a hollow) and adding the corresponding contributions.

2.4. **Further comments**

- We decided here to compute ourselves the electromagnetic field in order to be able to use its gradient explicitely in the expression of the gradient of the functional. Of course, we have done a validation of our computations by comparison with commercial codes (*Ampere* and *Ansys*).
- As explained in the Introduction, we have chosen a boundary element method to solve problems (7) and (32). More precisely, we use a Galerkin method to solve the integral equations (11), by multiplying both sides by basis functions defined on the mesh and integrating over the boundary. The choice of this formulation is motivated by the fact that these problems are set in exterior domains. Moreover, it has another advantage. In the different steps of our algorithm, the magnet is modified, but this modification occurs only in the right-hand side of the linear equations we have to solve. More precisely, the matrix of the linear system obtained in the Galerkin procedure is the same, not only for the state and the adjoint equation at one step, but at every step. Therefore, we can write a LU decomposition of this matrix at the beginning of the procedure, each resolution of the state or the adjoint equation being very fast after.
- It is well known in boundary element methods that we have to compute, after discretization, some singular integrals due to the kernel $\frac{1}{|X-Y|}$ in the integral equation (11). We circumvent this difficulty by transforming these integrals, thanks to an integration by part, into boundary integrals (on the boundary of each triangle).
- The optimization algorithm that we used is the by-now classical Quasi-Newton BFGS methods (see *e.g.* [2, 6]). We do the one-dimensional search with some steps of parabolic interpolation.
- The penalization parameter r for the volume constraint is not fixed, but adaptative. It changes dynamically during the procedure.
- During the procedure, the mesh of the magnet is, of course, modified. So we have to create new triangles. If the area of a triangle becomes too large, we decide to split it into three new triangles using the center of mass as a new node. We write a limitation on the angles in order to avoid creation of thin triangles. It is much more complicated to remove one triangle in a mesh, so we do not try to remove too small triangles.

3. Numerical results

We present the results for different initial geometries. First a table gives the values of the volume of the magnet and of the penalized functional after a certain number of iterations. The evolution of these quantities is also given in percentage. We have chosen to present the penalized functional, actually the penalization constant is adapted in such a way that the penalization term does not exceed 1% of the total functional. Then, we plot these relatives evolutions on a graphic. The solid line represents the penalized functional and the dashed line the volume. At last, we show three pictures of magnets.

3.1. **Parallelepiped**

Iterations	**Volume**	**% Volume**	**Functional**	**% Functional**
1	7.99	0	6.78×10^7	0
50	7.98	–0.31	7.19×10^7	6.09
100	8.00	0.03	7.44×10^7	9.77
150	8.04	0.46	7.75×10^7	14.35

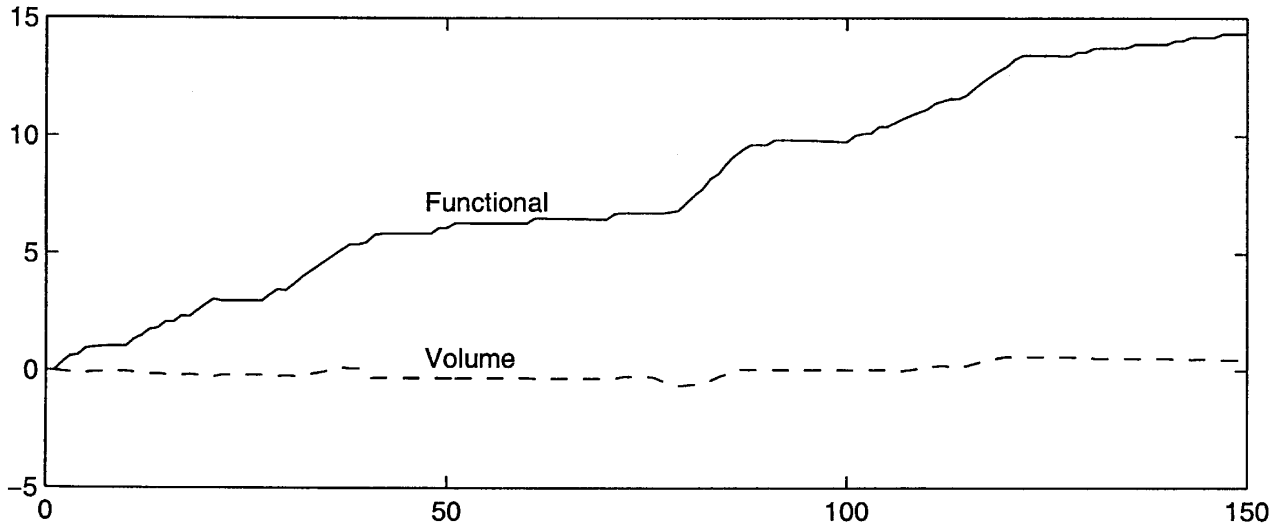

FIGURE 2. Evolution of the functional and the volume in percentage.

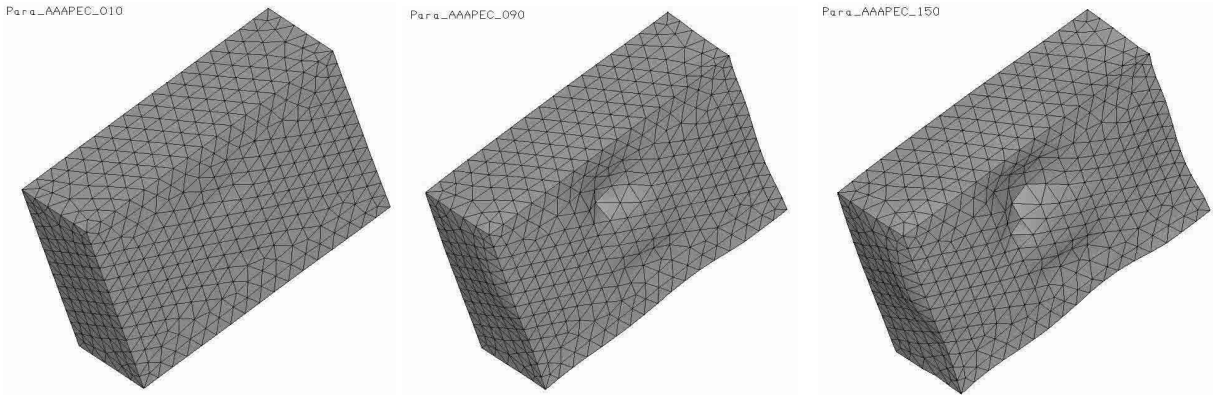

FIGURE 3. Magnet after 10 iterations (left), 90 iterations (center), 150 iterations (right).

3.2. **Cylinder**

Iterations	**Volume**	**% Volume**	**Functional**	**% Functional**
1	7.99	0	5.02×10^7	0
50	7.95	–0.51	5.32×10^7	5.99
100	7.93	–0.71	5.58×10^7	11.17
150	7.95	–0.54	5.83×10^7	16.20

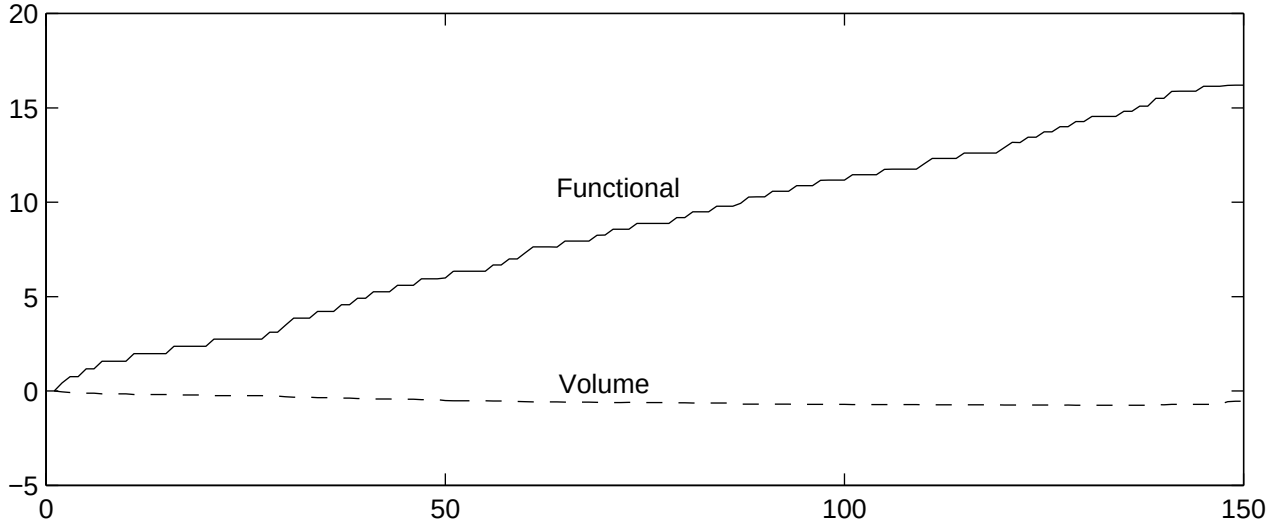

FIGURE 4. Evolution of the functional and the volume in percentage.

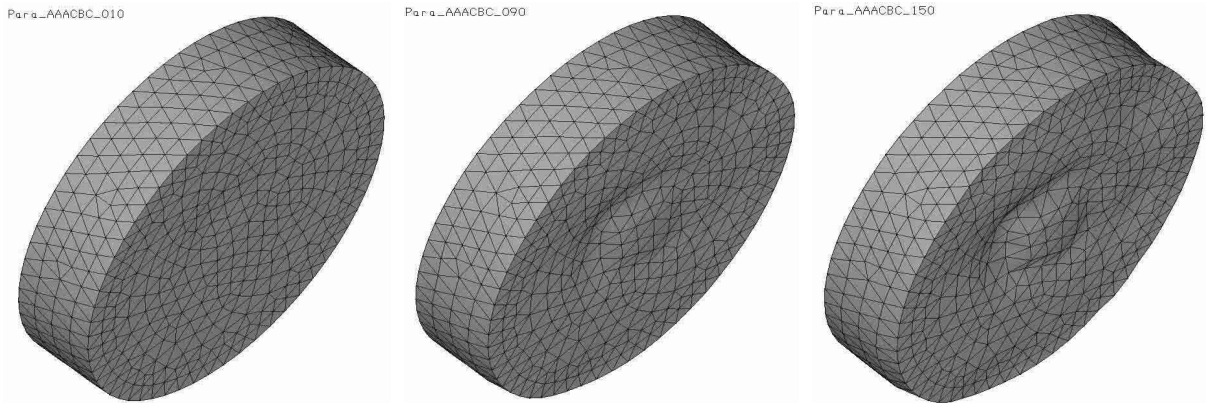

FIGURE 5. Magnet after 10 iterations (left), 90 iterations (center), 150 iterations (right).

3.3. **Bridge shape**

Iterations	**Volume**	**% Volume**	**Functional**	**% Functional**
1	8.00	0	1.03×10^4	0
10	7.91	–1.05	1.77×10^4	72.2
20	7.86	–1.76	2.06×10^4	99.8
25	7.83	–2.11	2.25×10^4	118.9

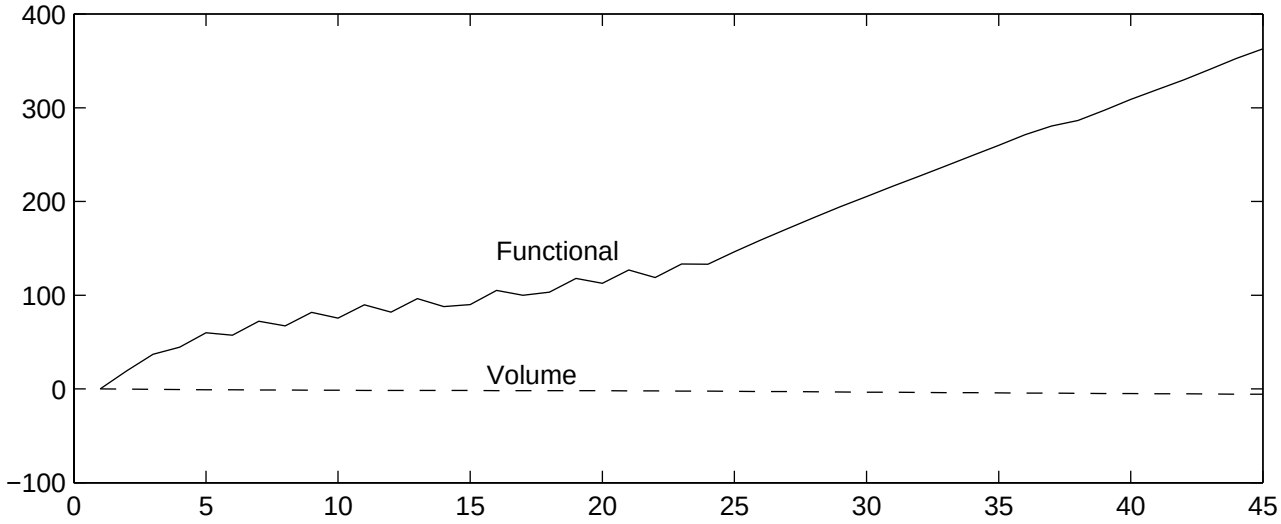

FIGURE 6. Evolution of the functional and the volume in percentage.

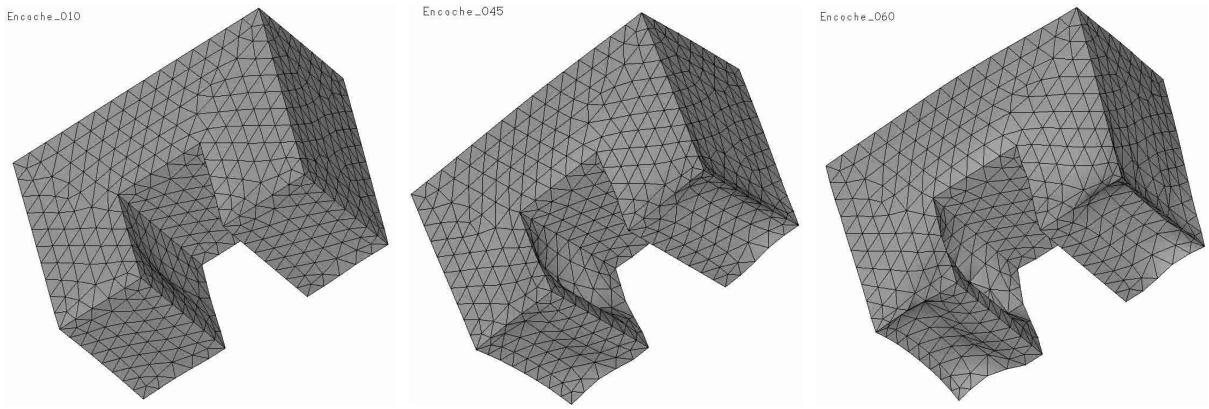

FIGURE 7. Magnet after 10 iterations (left), 45 iterations (center), 60 iterations (right).

3.4. **Final comments**

The above results show the efficiency of our method. Nevertheless, we were not able to observe convergence of the algorithm in any case. The main reason is that, after a certain number of steps, the mesh of the magnet is so deformed that some interpenetration or overlapping can occur. It is well visible in Figures 6 and 7. For this last case, we can see that the results are no longer valids after iteration 25 due to problems in the magnet's mesh. We believe that the above pictures are still far from the optimum. If we really would try to improve our method to study the convergence of our algorithm, we would need a clever way to remesh the magnets. We did not do it by lack of time.

As we could guess, in each example, the top of the magnet is not changed. Modifications only occur on the bottom and the lateral faces. It also appears a kind of bulge. It looks as if the magnet would try to mimic the toothed wheel.

References

[1] S. Agmon, *Lectures on Elliptic Boundary Value Problems*. Van Nostrand Math Studies (1965).
[2] J. Baranger, *Analyse Numérique*. Hermann, Paris (1991).
[3] D. Chenais, On the existence of a solution in a domain identification problem. *J. Math. Anal. Appl.* **52** (1975) 189–289.
[4] D. Chenais, Sur une famille de variétés à bord lipschitziennes, application à un problème d'identification de domaine. *Ann. Inst. Fourier* (Grenoble) **4** (1977) 201–231.
[5] R. Dautray and J.L. Lions (Eds.), *Analyse mathématique et calcul numérique*, Vol. I and II. Masson, Paris (1984).
[6] J.E. Dennis and R.B. Schnabel, *Numerical Methods for unconstrained optimization*. Prentice Hall (1983).
[7] E. Durand, *Magnétostatique*. Masson, Paris (1968).
[8] A. Henrot and M. Pierre, *Optimisation de forme* (to appear).
[9] M. Pierre and J.R. Roche, Computation of free sufaces in the electromagnetic shaping of liquid metals by optimization algorithms. *Eur. J. Mech. B Fluids* **10** (1991) 489–500.
[10] M. Pierre and J.R. Roche, Numerical simulation of tridimensional electromagnetic shaping of liquid metals. *Numer. Math.* **65** (1993) 203–217.
[11] O. Pironneau, *Optimal shape design for elliptic systems*. Springer Series in Computational Physics. Springer, New York (1984).
[12] J. Simon, Differentiation with respect to the domain in boundary value problems. *Numer. Funct. Anal. Optim.* **2** (1980) 649–687.
[13] J. Simon, *Variations with respect to domain for Neumann condition*. Proceedings of the 1986 IFAC Congress at Pasadena "Control of Distributed Parameter Systems".
[14] J. Sokolowski and J.P. Zolesio, *Introduction to shape optimization: shape sensitity analysis*. Springer Series in Computational Mathematics, Vol. 10, Springer, Berlin (1992).